Inorg. Chem. **2005**, *44*, 4983–4991

Directed Supramolecular Assembly of Infinite 1-D M(II)-Containing Chains (M = Cu, Co, Ni) Using Structurally Bifunctional Ligands

Christer B. Aakeröy,* Nate Schultheiss, and John Desper

Department of Chemistry, Kansas State University, Manhattan, Kansas 66506

Received November 12, 2004

The directed assembly of six different M(II) complexes (M = Cu, Co, and Ni) into infinite chains has been achieved by combining anionic chelating ligands (for controlling the coordination geometry) with bifunctional ligands containing a metal-coordinating pyridyl moiety and a self-complementary hydrogen-bonding moiety. Six crystal structures are presented, and in each case, the chelating acac ligand occupies the four equatorial coordination sites leaving room for the bifunctional ligand to coordinate in the axial positions. The supramolecular chemistry, which organizes the coordination complexes into the desired infinite 1-D chains, is driven by a combination of N–H···N and N–H···O hydrogen bonds.

Introduction

The directed assembly of coordination complexes into discrete entities or extended networks with predictable connectivity and dimensionality remains a particularly challenging task.[1] However, using assembly strategies based upon coordinate-covalent bonds, a multitude of metal ions in a variety of oxidation states and with different coordination environments have been incorporated into coordination polymers[2] or metallacycles[3] that may become useful as catalysts[4] or in magnetic,[5] optical,[6] or electronic[7] devices. Considerably less attention has been focused on producing extended metal-containing motifs where the assembly and organization of neighboring complex ions is driven by weaker noncovalent interactions such as hydrogen bonds, $\pi-\pi$ interactions, etc.[8] Since the physical properties of any solid are strongly influenced by the communication and interactions between molecules or complex ions, it is important, from the point of view of tuning the properties, to be able to alter specific metrics (e.g. distance between metal ions) without inducing dramatic changes to the overall crystal structure. Thus, the design of versatile bifunctional ligands that are capable of coordinating to a metal ion while providing the means for organizing such complex ions into extended networks in a predictable manner is an important aspect of current structural inorganic chemistry.

We are specifically interested in developing reliable and versatile supramolecular routes for the directed assembly of metal ions into infinite 1-D chains to gain some control over metal−metal distances within extended chains. To reach this specific supramolecular goal it is important that the synthetic

* Author to whom correspondence should be addressed. E-mail: aakeroy@ksu.edu.

(1) Braga, D.; Desiraju, G. R.; Miller, J. S.; Orpen, A. J.; Price, S. L. *CrystEngComm* **2002**, 500−509. (b) Tashiro, S.; Tominaga, M.; Kusukawa, T.; Kawano, M.; Sakamoto, S.; Yamaguchi, K.; Fujita, M. *Angew. Chem., Int. Ed*. **2003**, *42*, 3267−3270. (c) Natarajan, R.; Savitha, G.; Moorthy, J. N. *Cryst. Growth Des*. **2004**, ASAP.

(2) (a) Berry, J. F.; Cotton, F. A.; Murillo, C. A. *Inorg. Chim. Acta* **2004**, *357*, 3847−3853. (b) Berry, J. F.; Cotton, F. A.; Fewox, C. S.; Lu, T.; Murillo, C. A.; Wang, X. *Dalton Trans*. **2004**, *15*, 2297−2302. (c) McManus, G. J.; Wang, Z.; Zaworotko, M. J. *Cryst. Growth Des*. **2004**, *4*, 11−13.

(3) (a) Chatterjee, B.; Noveron, J. C.; Resendiz, M.; Liu, J.; Yamamoto, T.; Parker, D.; Cinke, M.; Nguyen, C. V.; Arif, A. M.; Stang, P. J. *J. Am. Chem. Soc*. **2004**, *126*, 10645−10656. (b) Mukherjee, P. S.; Das, N.; Kryschenko, Y. K.; Arif, A. M.; Stang, P. J. *J. Am. Chem. Soc*. **2004**, *126*, 2464−2473. (c) Berry, J. F.; Cotton, F. A.; Murillo, C. A. *Inorg. Chem. Acta* **2004**, *357*, 3847−3853.

(4) (a) Walker, S. D.; Barder, T. E.; Martinelli, J. R.; Buchwald, S. L. *Angew. Chem., Int. Ed*. **2004**, *43*, 1871−1876. (b) Strieter, E. R.; Blackmond, D. G.; Buchwald, S. L. *J. Am. Chem. Soc.* **2003**, *125*, 13978−13980. (c) Ohmori, O.; Fujita, M. *Chem. Commun*. **2004**, *14*, 1586−1587.

(5) (a) Kahn, O. *Acc. Chem. Res*. **2000**, *33*, 1−11. (b) Chapman, M. E.; Ayyappan, P.; Foxman, B. M.; Yee, G. T.; Lin, W. *Cryst. Growth Des.* **2001**, *2*, 159−163. (c) Berry, J. F.; Cotton, F. A.; Lei, P.; Murillo, C. A. *Inorg. Chem.* **2003**, *42*, 377−382.

(6) (a) Cariati, F.; Caruso, U.; Centore, R.; Marcolli, W.; Maria, A. D.; Panunzi, B.; Roviello, A.; Tuzi, A. *Inorg. Chem.* **2002**, *41*, 6597−6603. (b) Noveron, J. C.; Arif, A. M.; Stang, P. *J. Chem. Mater*. **2003**, *15*, 372−374. (c) Hou, H.; Song, Y.; Xu, H.; Wei, Y.; Fan, Y.; Zhu, Y.; Li, L.; Du, C. *Macromolecules* **2003**, *36*, 999−1008.

(7) (a) Laitar, D. S.; Mathison, C. J. N.; Davis, W. M.; Sadighi, J. P. *Inorg. Chem*. **2003**, *42*, 7354−7356. (b) Gumienna-Kontecka, E.; Rio, Y.; Bourgogne, C.; Elhabiri, M.; Louis, R.; Albrecht-Gary, A.-M.; Nierengarten, J.-F. *Inorg. Chem*. **2004**, *43*, 3200−3209.

(8) (a) Aakeröy, C. B.; Beatty, A. M.; Lorimer, K. R. J. *Chem. Soc., Dalton Trans*. **2000**, 3869−3872. (b) Aakeröy, C. B.; Beatty, A. M.; Leinen, D. S.; Lorimer, K. R. J. *Chem. Commun*. **2000**, 935−936. (c) Aakeröy, C. B.; Beatty, A. M.; Desper, J.; O'Shea, M.; Valdés-Martínez, J. *Dalton Trans*. **2003**, 3956−3962. (d) Bose, D.; Banerjee, J.; Rahaman, S. H.; Mostafa, G.; Fun, H.-K.; Bailey Walsh, R. D.; Zaworotko, M. J.; Ghosh, B. K. *Polyhedron* **2004**, *23*, 2045−2053.

10.1021/ic048405y CCC: $30.25
Published on Web 06/16/2005

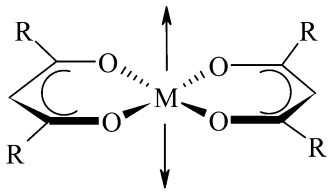

R = CF_3, Phenyl
M = Cu, Co, Ni

Figure 1. Substituted acac complex with the arrows showing the two axial coordination sites.

process is designed such that the number of potentially structurally interfering components present, or introduced, during the assembly process is kept to a minimum. In essence, the reaction conditions need to be optimized in the same way that reaction conditions for covalent synthesis are selected for maximum yield.

The yield (i.e. frequency of occurrence of a desired structural motif) for a set of supramolecular reactions involving coordination complexes can be improved by ensuring that the coordination number/geometry for the metal ion is strictly controlled and that the need for potentially disruptive counterions is eliminated. With this in mind, we decided to employ copper(II) 1,1,1,5,5,5-hexafluoro-2,4-pentanedione [$(hfac)_2Cu^{II}$], cobalt(II) 1,3-diphenyl-1,3-propanedione [$(DBM)_2Co^{II}$], and nickel(II) 1,3-diphenyl-1,3-propanedione [$(DBM)_2Ni^{II}$] complexes as starting points for this study.[9] Complexes of this type are attractive due to the fact that two dione anions occupy four equatorial sites around the M(II) ion thereby producing an overall neutral metal-containing building block. In addition, the two remaining axial sites can be utilized for constructing extended linear supramolecular architectures with an appropriate bifunctional ligand, Figure 1.

A suitable bifunctional ligand would contain a chemical functionality with the capability of binding to metal ions, e.g. a pyridyl moiety, coupled with a functional group that can interact with a neighboring ligand through self-complementary hydrogen bonds. With these requirements in mind, we decided to target the coordination chemistry of three new ligands, **1**, **2**, and **6**, Figure 2. **1** and **2** have slightly different sterics and electronics in the vicinity of the hydrogen-bonding functionality, whereas **6** incorporates an ethynyl linker between the pyridyl and the aminopyrimidine units. This ethynyl bridge elongates the ligand allowing for even further extension between metal centers, and it is important to establish if hydrogen-bond interactions can maintain sufficient structural influence even to the point of organizing larger coordination complexes into desired extended motifs.

In this paper we present the design and synthesis of three new bifunctional ligands, Figure 2, and the six crystal

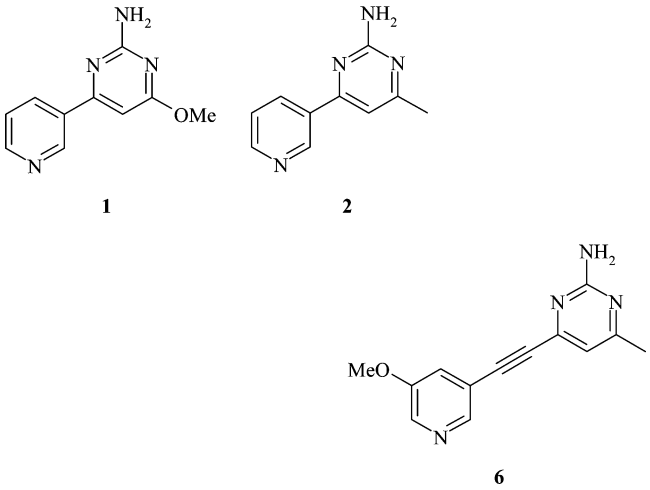

Figure 2. Bifunctional ligands, 3-(2-amino-4-methoxypyrimidin-6-yl)-pyridine, **1**, 3-(2-amino-4-methylpyrimidin-6-yl)pyridine, **2**, and 1-(2-amino-4-methylpyrimidin-6-yl)-2-(3-methoxypyridin-5-yl)ethyne, **6**.

structures that were obtained when they were allowed to react with [$(hfac)_2Cu^{II}$], [$(DBM)_2Co^{II}$], or [$(DBM)_2Ni^{II}$] resulting in infinite inorganic:organic networks. The structures are analyzed and discussed in the context of the relevant supramolecular design strategies and structural targets.

Experimental Section

Synthesis. All chemicals were purchased from Aldrich and used without further purification.

3-(2-Amino-4-methoxypyrimidin-6-yl)pyridine, 1. A mixture of 2-amino-4-chloro-6-methoxypyrimidine (1.50 g, 9.38 mmol), 3-pyridylboronic acid[10] (1.58 g, 10.33 mmol), sodium carbonate (0.700 g, 6.6 mmol), and bis(triphenylphosphine)palladium(II) dichloride (180 mg, 0.256 mmol, 2.7 mol %) was added to a round-bottom flask. Acetonitrile (35 mL) and water (35 mL) were added, and dinitrogen was bubbled through the resultant mixture for 10 min. A condenser was attached and the mixture heated at 75 °C under a dinitrogen atmosphere. The reaction was monitored by TLC and allowed to cool to room temperature on completion (12 h). The solution was then diluted with 150 mL of ethyl acetate, washed with water (3 × 100 mL), and then washed with saturated aqueous sodium chloride (2 × 100 mL). The organic layer was separated and dried over magnesium sulfate. The solvent was removed on a rotary evaporator and the residue chromatographed on silica with a hexanes/ethyl acetate mixture (1:1) as the eluant. The product was isolated as a white solid. The product **1** was then recrystallized from ethanol (200 proof) as colorless hair-shaped crystals (1.44 g, 76%). Mp: 138−140 °C. ^{1}H NMR (δ_H; 400 MHz, $CDCl_3$): 9.15 (d, $J = 2.4$ Hz, 1H), 8.68 (dd, $J = 4$ Hz, $J = 1$ Hz, 1H), 8.25 (dt, $J = 8.8$ Hz, $J = 2.4$ Hz, 1H), 7.38 (dd, $J = 8$ Hz, $J = 4.8$ Hz, 1H), 6.52 (s, 1H), 5.09 (s, 2H), 3.95 (s, 3H). ^{13}C NMR (δ_C; 400 MHz, $CDCl_3$): 171.61, 163.34, 163.21, 150.87, 148.38, 134.28, 133.15, 123.37, 94.387, 53.51. IR (KBr): 3451, 3354, 1582, 1362 cm^{-1}.

(9) (a) Panthou, F. L.; Luneau, D.; Musin, R.; Öhrström, L.; Grand, A.; Turek, P.; Rey, P. *Inorg. Chem.* **1996**, *35*, 3484−3491. (b) Sano, Y.; Tanaka, M.; Koga, N.; Matsuda, K.; Iwamura, H.; Rabu, P.; Drillon, M. *J. Am. Chem. Soc.* **1997**, *119*, 8246−8252.

(10) Li, W.; Nelson, D. P.; Jensen, M. S.; Hoerner, R. S.; Cai, D.; Larsen, R. D.; Reider, P. J. *J. Org. Chem.* **2002**, *67*, 5394−5397.

3-(2-Amino-4-methylpyrimidin-6-yl)pyridine, 2. A similar procedure was followed for the methyl derivative. Column chromatography was carried out with a hexanes/ethyl acetate mixture (1:4) as the eluant and the product **2** recrystallized from ethanol/chloroform as colorless block-shaped crystals yielding 74%. Mp: 192−194 °C. ^{1}H NMR (δ_H; 400 MHz, DMSO-d_6): 9.18 (d, J = 2 Hz, 1H), 8.63 (dd, J = 4.8 Hz, J = 1.6 Hz, 1H), 8.33 (dt, J = 8 Hz, J = 1.6 Hz, 1H), 7.48 (dd, J = 8 Hz, J = 4.8 Hz, J = 0.8 Hz, 1H), 7.09 (s, 1H), 6.65 (s, 2H), 2.28 (s, 3H). ^{13}C NMR (δ_C; 400 MHz, DMSO-d_6): 168.52, 163.61, 161.43, 150.88, 147.89, 134.05, 132.66, 123.64, 105.41, 23.66. IR (KBr): 3324, 3154, 1576, 1345 cm^{-1}.

3-Methoxy-5-bromopyridine, 3. A solution of sodium methoxide in 25% methanol (6.83 mL, 31.6 mmol) was combined with DMF (anhydrous 20 mL) under an inert N_2 atmosphere in a round-bottom flask. 3,5-Dibromopyridine (5.00 g, 21.1 mmol) was then added and stirred at 65 °C for 24 h. An additional 1 equiv of sodium methoxide in 25% methanol (2.33 mL) was added after 4 h. The reaction was monitored by TLC and allowed to cool to room temperature upon completion. The reaction was then diluted with water (50 mL) and extracted with diethyl ether (3 × 50 mL). The organic extractions were combined and washed with brine and then dried over magnesium sulfate. The solvent was removed on a rotary evaporator and the residue chromatographed on silica with a hexanes/ethyl acetate mixture (1:1) as the eluant. The product, 5-bromo-3-methoxypyridine,[11] was isolated as a yellow oil. Hexanes (20 mL) was then added to the product, and the solution was placed in the refrigerator. Colorless crystals precipitated from the mother liquor, which were isolated and dried (2.82 g, 71%). Mp: 27−29 °C. ^{1}H NMR (δ_H; 400 MHz, $CDCl_3$): 8.29 (d, J = 1.6 Hz, 1H), 8.25 (d, J = 2.4 Hz, 1H), 7.36 (dd, J = 2.6 Hz, J = 1.8 Hz, 1H), 3.86 (s, 3H). ^{13}C NMR (δ_C; 400 MHz, $CDCl_3$): 155.83, 142.70, 136.01, 123.01, 120.18, 55.61.

3-Methoxy-5-((trimethylsilanyl)ethynyl)pyridine, 4. 3-Methoxy-5-bromopyridine (3.26 g, 17.31 mmol), (trimethylsilyl)acetylene (2.05 g, 20.9 mmol), copper(I) iodide (0.100 g, 0.590 mmol), triphenylphosphine (0.420 g, 1.60 mmol), and bis(triphenylphosphine)palladium(II) dichloride (0.360 g, 0.510 mmol) were added to a round-bottom flask. Tetrahydrofuran (75 mL) and triethylamine (75 mL) were added, and dinitrogen was bubbled through the resultant mixture for 10 min. A condenser was attached and the mixture heated at 65 °C under a dinitrogen atmosphere. The reaction was monitored by TLC and allowed to cool to room temperature on completion (26 h). The solution was then diluted with 100 mL of ethyl acetate, and the new solution was washed with water (3 × 100 mL) and then washed with saturated aqueous sodium chloride (1 × 100 mL). The organic layer was separated and dried over magnesium sulfate. The solvent was removed on a rotary evaporator and the residue chromatographed on silica with *n*-pentane as the eluant. The product **4** was isolated as a light yellow oil (4.25 g, 86%). ^{1}H NMR (δ_H; 200 MHz, $CDCl_3$): 8.27 (d, 1.6 Hz, 1H), 8.21 (d, J = 5.2 Hz, 1H), 7.20 (dd, J = 6 Hz, J = 2.8, 1H), 3.81 (s, 3H), 0.24 (s, 9H).

3-Methoxy-5-ethynylpyridine, 5. A mixture of 3-methoxy-5-((trimethylsilanyl)ethynyl)pyridine (4.25 g, 14.9 mmol) and potassium carbonate (3.00 g, 21.7 mmol) was stirred in methanol (80 mL) at room temperature for 1 h. The solution was then diluted with ethyl ether (100 mL) and washed with water (4 × 100 mL). The solvent was removed on a rotary evaporator and the residue chromatographed on silica with a *n*-pentane/ethyl acetate (10:1) as eluant. The product **5** was isolated as a white solid (1.72 g, 87%). ^{1}H NMR (δ_H; 200 MHz, $CDCl_3$): 8.21 (d, J = 2.8 Hz, 1H), 8.16 (d, J = 4 Hz, 1H), 7.15 (dd, J = 5.8 Hz, J = 3 Hz, 1H), 3.72 (s, 3H), 3.17 (s, 1H).

1-(2-Amino-4-methylpyrimidin-6-yl)-2-(3-methoxypyridin-5-yl)ethyne, 6. 2-Amino-4-chloro-6-methylpyrimidine (360 mg, 2.50 mmol), 3-methoxy-5-ethynylpyridine (400 mg, 3.01 mmol), copper(I) iodide (12.0 mg, 0.0710 mmol), triphenylphosphine (50.0 mg, 0.191 mmol), and bis(triphenylphosphine)palladium(II) dichloride (50.0 mg, 0.071 mmol) were added to a round-bottom flask. Tetrahydrofuran (12 mL) and triethylamine (12 mL) were added, and dinitrogen was bubbled through the resultant mixture for 10 min. A condenser was attached and the mixture heated at 70 °C under a dinitrogen atmosphere. The reaction was monitored by TLC and allowed to cool to room temperature upon completion (48 h). The solution was then diluted with 50 mL of ethyl acetate, and the new solution was washed with water (3 × 100 mL) and then washed with saturated aqueous sodium chloride (1 × 100 mL). The organic layer was separated and dried over magnesium sulfate. The solvent was removed on a rotary evaporator and the residue chromatographed on silica with a hexanes/ethyl acetate mixture (1:1) as the eluant. The product **6** was isolated as a light brown solid. The product was recrystallized from chloroform producing colorless block-shaped crystals (426 mg, 72%). Mp: 171−173 °C. ^{1}H NMR (δ_H; 400 MHz, $CDCl_3$): 8.39 (d, J = 2 Hz, 1H), 8.30 (d, J = 2.8 Hz, 1H), 7.36 (dd, J = 3 Hz, J = 1.4 Hz, 1H), 6.70 (s, 1H), 5.43 (s, 2H), 3.85 (s, 3H), 2.35 (s, 3H). ^{13}C NMR (δ_C; 400 MHz, $CDCl_3$): 168.88, 162.83, 154.99, 150.37, 144.92, 138.72, 122.61, 118.80, 113.48, 89.78, 87.66, 55.60, 23.81. IR (KBr): 3326, 3171, 2229, 1652, 1558, 1423 cm^{-1}.

2:1 Complex of 3-(2-Amino-4-methoxypyrimidin-6-yl)-pyridine with Copper(II) 1,1,1,5,5,5-Hexafluoro-2,4-pentanedione, 7. 3-(2-Amino-4-methoxypyrimidin-6-yl)pyridine (13 mg, 0.060 mmol) and copper(II) 1,1,1,5,5,5-hexafluoro-2,4-pentanedione (17 mg, 0.040 mmol) were added to a screw cap vial along with chloroform (3 mL). The mixture was heated gently until a clear homogeneous solution resulted. Green prism-shaped crystals were harvested after 3 days (13 mg, 46%). Mp: 143−145 °C.

2:1 Complex of 3-(2-Amino-4-methoxypyrimidin-6-yl)-pyridine with Cobalt(II) 1,3-Diphenyl-1,3-propanedione, 8. 3-(2-Amino-4-methoxypyrimidin-6-yl)pyridine (12 mg, 0.060 mmol) and cobalt(II) 1,3-diphenyl-1,3-propanedione (16 mg, 0.030 mmol) were added to a screw cap vial along with a mixture of 1,2-dichloroethane/chloroform (7:3 mL).

(11) Comins, D. L.; Killpack, M. O. *J. Org. Chem.* **1990**, *55*, 69−73.

Table 1. Crystallographic Data for Compounds **7**−**12**

	7	**8**	**9**
systematic name	bis(1,1,1,5,5,5-hexafluoro-2,4-pentanedionato)-bis[3-(2-amino-6-methoxypyrimidin-4-yl)-pyridyl]copper(II)−2-chloroform	bis(1,3-diphenyl-1,3-propanedionato)-bis[3-(2-amino-6-methoxypyrimidin-4-yl)-pyridyl]cobalt(II)	bis(1,1,1,5,5,5-hexafluoro-2,4-pentanedionato)-bis[3-(2-amino-6-methyl-pyrimidin-4-yl)-pyridine]copper(II)−1,2-di-chloroethane
formula moiety	$(C_5HF_6O_2)_2(C_{10}H_{10}N_4O)_2Cu{\cdot}2CHCl_3$	$(C_{15}H_{11}O_2)_2(C_{10}H_{10}N_4O)_2Co$	$(C_5HF_6O_2)_2(C_{10}H_{10}N_4)_2Cu{\cdot}C_2H_4Cl_2$
empirical formula	$C_{32}H_{24}Cl_6CuF_{12}N_8O_6$	$C_{50}H_{42}CoN_8O_6$	$C_{32}H_{26}Cl_2CuF_{12}N_8O_4$
M_r	1120.83	909.85	949.05
color, habit	green prism	yellow prism	blue-green block
space group, Z	$P\bar{1}$, 2	$P\bar{1}$, 1	$P\bar{1}$, 1
a, Å	10.4149(6)	9.3368(7)	8.2843(4)
b, Å	12.1682(7)	10.3686(8)	10.8750(5)
c, Å	18.2488(10)	11.0609(8)	11.7573(6)
α, deg	105.6980(10)	85.536(2)	113.0810(10)
β, deg	105.8970(10)	79.677(2)	94.4120(10)
γ, deg	93.1160(10)	83.026(2)	103.8330(10)
V, Å^3	2120.6(2)	1043.95(14)	928.75(8)
density, g/cm^3	1.755	1.447	1.697
temp, K	100(2)	100(2)	100(2)
X-ray wavelength, Å	0.710 73	0.710 73	0.710 73
μ, mm^{-1}	1.000	0.475	0.843
θ_{min}, deg	1.76	1.87	2.13
θ_{max}, deg	30.00	30.00	30.03
reflcns			
collcd	24 652	12 145	10 734
indpndnt	12 133	5980	5322
obsd	9791	5233	4874
threshold expression	$>2\sigma(I)$	$>2\sigma(I)$	$>2\sigma(I)$
R_1(obsd)	0.0459	0.0462	0.0376
wR_2(all)	0.1263	0.1121	0.1077
T_{min}	0.834	0.79	0.816
R_{merge}, %	2.57	2.28	1.6

	10	**11**	**12**
systematic name	bis(1,1,1,5,5,5-hexafluoro-2,4-pentanedionato)-[1-(2-amino-4-methylpyrimidin-6-yl)-2-(3-methoxypyridin-5-yl)ethyne]copper(II)	bis(1,3-diphenyl-1,3-propanedionato)-bis[1-(2-amino-4-methylpyrimidin-6-yl)-2-(3-methoxypyridin-5-yl)ethyne]cobalt(II)	bis(1,3-diphenyl-1,3-propanedionato)-bis[1-(2-amino-4-methylpyrimidin-6-yl)-2-(3-methoxypyridin-5-yl)-ethyne]nickel(II)
formula moiety	$(C_5HF_6O_2)_2(C_{13}H_{12}N_4O)Cu$	$(C_{13}H_{12}N_4O)_2(C_{15}H_{11}O_2)_2\,Co$	$(C_{15}H_{11}O_2)_2(C_{13}H_{12}N_4O)_2Ni$
empirical formula	$C_{23}H_{14}CuF_{12}N_4O_5$	$C_{56}H_{46}CoN_8O_6$	$C_{56}H_{46}N_8NiO_6$
M_r	717.92	985.94	985.72
color, habit	green block	orange block	green plate
space group, Z	$P\bar{1}$, 2	$P\bar{1}$, 1	$P\bar{1}$, 1
a, Å	9.6243(11)	10.5076(5)	10.4666(7)
b, Å	10.4481(12)	10.7568(6)	10.6669(7)
c, Å	13.8822(15)	11.9544(6)	11.9828(8)
α, deg	85.905(2)	68.9160(10)	68.678(4)
β, deg	86.300(2)	82.6200(10)	82.626(4)
γ, deg	74.690(2)	69.1900(10)	69.230(3)
V, Å^3	1341.4(3)	1178.48(10)	1165.27(13)
density, g/cm^3	1.777	1.389	1.405
temp, K	100(2)	100(2)	173(2)
X-ray wavelength, Å	0.710 73	0.710 73	0.710 73
μ, mm^{-1}	0.941	0.427	0.480
θ_{min}, deg	2.02	2.07	1.82
θ_{max}, deg	30.08	30.02	27.84
reflcns			
collcd	15 237	13 759	11 668
indpndnt	7644	6762	5170
obsd	6241	6106	3767
threshold expression	$>2\sigma(I)$	$>2\sigma(I)$	$>2\sigma(I)$
R_1(obsd)	0.0467	0.0429	0.0570
wR_2(all)	0.1333	0.1111	0.1470
T_{min}	0.698	0.823	no abs corr
R_{merge}, %	2.60	2.38	12.4

The mixture was heated gently until a clear homogeneous solution resulted. Orange prism-shaped crystals formed after 1 day (19 mg, 70%). Mp: 219 °C (dec).

2:1 Complex of 3-(2-Amino-4-methylpyrimidin-6-yl)-pyridine with Copper(II) 1,1,1,5,5,5-Hexafluoro-2,4-pentanedione, 9. 3-(2-Amino-4-methylpyrimidin-6-yl)pyridine (14 mg, 0.080 mmol) and copper(II) 1,1,1,5,5,5-hexafluoro-2,4-pentanedione (18 mg, 0.040 mmol) were added to a screw cap vial along with 1,2-dichloroethane (4 mL). The mixture was heated gently until a clear homogeneous solution resulted. Green block-shaped crystals were collected after 2 days (18 mg, 56%). Mp: 156−158 °C.

1:1 Complex of 1-(2-Amino-4-methylpyrimidin-6-yl)-2-(3-methoxypyridin-5-yl)ethyne with Copper(II) 1,1,1,5,5,5-Hexafluoro-2,4-pentanedione, 10. 1-(2-Amino-4-methylpyrimidin-6-yl)-2-(3-methoxypyridin-5-yl)ethyne (9.0 mg, 0.040

Table 2. Selected Hydrogen Bond Lengths, Å, and Angles, deg, for Compounds **7**−**12**

7	N(27)−H(27B)···O(34)$^{\#3\,a}$	0.88	2.25	3.112(2)	165.5
	N(57)−H(57B)···O(62)$^{\#4\,a}$	0.88	2.19	3.040(2)	162.7
8	N(52)−H(52A)···N(51)$^{\#2\,b}$	0.86(2)	2.37(2)	3.203(2)	164(2)
	N(52)−H(52B)···O(13)$^{\#3\,b}$	0.88(2)	2.16(2)	3.0337(18)	171(2)
9	N(22)−H(22A)···N(21)$^{\#3\,c}$	0.80(3)	2.28(3)	3.0847(19)	174(2)
10	N(12)−H(12A)···N(11)$^{\#1\,d}$	0.88	2.12	3.002(3)	175.0
	N(12)−H(12B)···O(42)$^{\#2\,d}$	0.88	2.27	3.044(2)	147.5
11	N(12)−H(12A)···O(31)$^{\#2\,e}$	0.87(2)	2.18(2)	3.0365(16)	169.1(18)
	N(12)−H(12B)···N(11)$^{\#3\,e}$	0.81(2)	2.26(2)	3.0656(17)	173.1(18)
12	N(22)−H(22A)···O(31)	0.78(3)	2.29(3)	3.058(3)	168(3)
	N(22)−H(22B)···N(21)$^{\#2\,f}$	0.82(3)	2.24(3)	3.058(3)	173(3)

^{a} (#3) $x, y-1, z$; (#4) $x, y+1, z$. ^{b} (#2) $-x+1, -y, -z$; (#3) $x, y, z-1$. ^{c} (#3) $-x+2, -y+1, -z+1$. ^{d} (#1) $-x+1, -y, -z+2$; (#2) $-x+1, -y+1, -z+1$. ^{e} (#2) $-x+1, -y+2, -z+1$; (#3) $-x, -y+3, -z$. ^{f} (#2) $-x, -y, -z'$.

mmol) and copper(II) 1,1,1,5,5,5-hexafluoro-2,4-pentanedione (10 mg, 0.020 mmol) were added to a screw cap vial along with chloroform (2 mL). Green block-shaped crystals were collected after 1 day (14 mg, 52%). Mp: 164−166 °C.

2:1 Complex of 1-(2-Amino-4-methylpyrimidin-6-yl)-2-(3-methoxypyridin-5-yl)ethyne with Cobalt(II) 1,3-Diphenyl-1,3-propanedione, 11. 1-(2-Amino-4-methylpyrimidin-6-yl)-2-(3-methoxypyridin-5-yl)ethyne (10 mg, 0.040 mmol) and cobalt(II) 1,3-diphenyl-1,3-propanedione (11 mg, 0.020 mmol) were added to a screw cap vial along with chloroform (2 mL). Orange block-shaped crystals were grown over a period of 1 day (13 mg, 65%). Mp: 215 °C (dec).

2:1 Complex of 1-(2-Amino-4-methylpyrimidin-6-yl)-2-(3-methoxypyridin-5-yl)ethyne with Nickel(II) 1,3-Diphenyl-1,3-propanedione, 12. 1-(2-Amino-4-methylpyrimidin-6-yl)-2-(3-methoxypyridin-5-yl)ethyne (10 mg, 0.04 mmol) and nickel(II) 1,3-diphenyl-1,3-propanedione (11 mg, 0.02 mmol) were added to a screw cap vial along with a mixture of nitromethane/dichloromethane (2:2 mL). Green plate-shaped crystals were grown over a period of 2 days (12 mg, 36%). Mp: 205 °C (dec).

X-ray Crystallography. Unless otherwise noted, X-ray data were collected on a Bruker SMART APEX three-circle CCD diffractometer using Mo Kα radiation. Data were collected using SMART.[12] Initial cell constants were found by small widely separated "matrix" runs. An entire hemisphere of reciprocal space was collected. All compounds in this study crystallized in the triclinic $P\bar{1}$ space group. Scan speed and scan width were chosen on the basis of scattering power and peak rocking curves. Unless otherwise noted, data were collected at −173 °C, using a 0.3° scan width.

Unit cell dimensions and the orientation matrix were improved by least-squares refinement of reflections "thresholded" from the entire dataset. Integration was performed with SAINT,[13] using this improved unit cell as a starting point. Precise unit cell dimensions were calculated in SAINT from the final merged dataset. Lorenz and polarization corrections were applied, and data were corrected for absorption. Data were reduced with SAINT.

Scheme 1

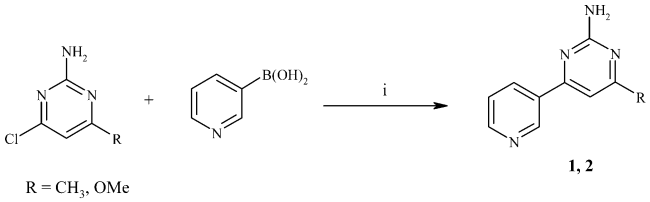

Scheme 2

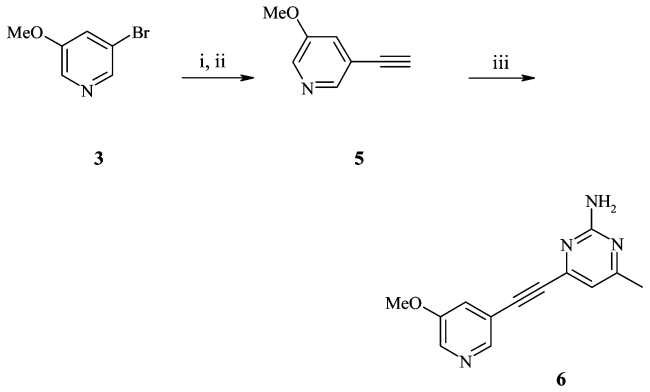

The structure was solved and refined with SHELXTL.[14] The structures were solved in all cases by direct methods without incident. In general, hydrogen atoms were assigned to idealized positions and were allowed to ride. Where possible, the coordinates of hydrogen-bonding hydrogen atoms were allowed to refine. Heavy atoms, other than those of the guests, were refined with anisotropic thermal parameters. Crystallographic details for each individual structure follows.

7. Two disordered chloroform sites were identified in the difference Fourier map. Two conformers were included for each site, with occupancy for each site set to sum to 1, with the minor conformer constrained to approximate the geometry of the major conformer, and with thermal parameters for similarly located atoms tied to each other. The lattice contains two complexes, each located on a crystallographic inversion center. Amine hydrogen atoms H27A, H27B, H57A, and H57B were included at calculated positions. Although the placement of these two species on special positions suggested the possibility of a sublattice, the chloroform molecules were not similarly positioned.

8. The cobalt complex sits on a crystallographic inversion center. Coordinates for the amine hydrogen atoms, H52A and H52B, were allowed to refine.

9. The asymmetric unit contains a copper complex, located on an inversion center, and a disordered 1,2-dichloroethane species. The latter species contained two conformers (in an approximately 85:15 mixture), both of which straddled an inversion center. The unique carbon on both species was refined isotropically. For purposes of connectivity tables, two chlorine atoms, sharing atomic coordinates and thermal

(12) *SMART*, v5.060; Bruker Analytical X-ray Systems: Madison, WI, 1997−1999.
(13) *SAINT*, v6.02; Bruker Analytical X-ray Systems: Madison, WI, 1997−1999.
(14) *SHELXTL*, v5.10; Bruker Analytical X-ray Systems: Madison, WI, 1997.

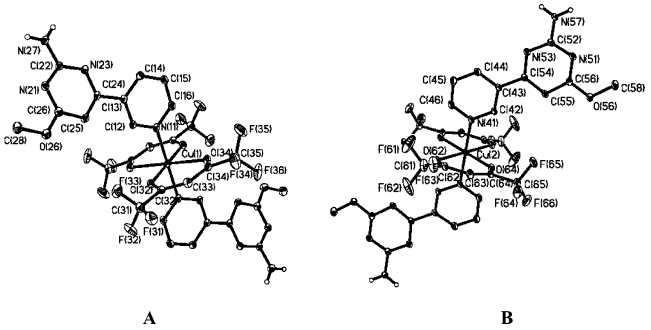

Figure 3. Labeled thermal ellipsoids (50% probability level) of the two asymmetric complex ions in the crystal structure of **7**. Two molecules of chloroform are omitted for clarity.

bit of $-CF_3$ disorder was modeled with two conformers (90:10 ratio). Geometry of the minor species was constrained to that of the major species, the isotropic thermal parameters of the two carbons were tied, and a free variable was employed to model isotropic thermal motion for the fluorine atoms on the minor conformer. Amine hydrogen atoms H12A and H12B were included in calculated positions.

11. The cobalt complex sits on a crystallographic inversion center. Amine hydrogen atoms H12A and H12B were allowed to refine.

12. Data were collected on a SMART 1000 CCD diffractometer at −100 °C, using a 0.2° scan width. The nickel complex sits on a crystallographic inversion center. Amine hydrogen atoms H22A and H22B were allowed to refine.

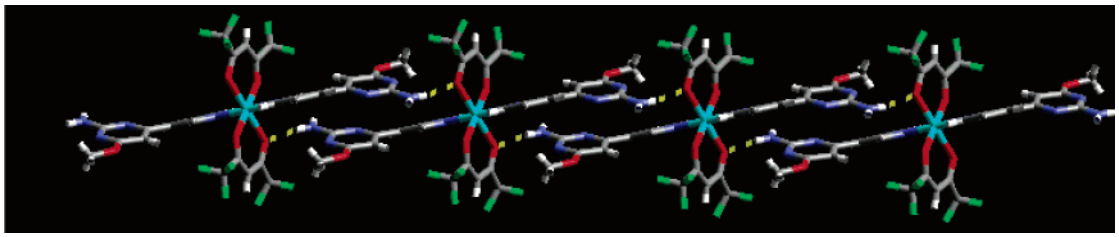

Figure 4. Adjacent complex ions in **7** organized into an extended chain held together by head-to-tail N−H···O hydrogen bonds.

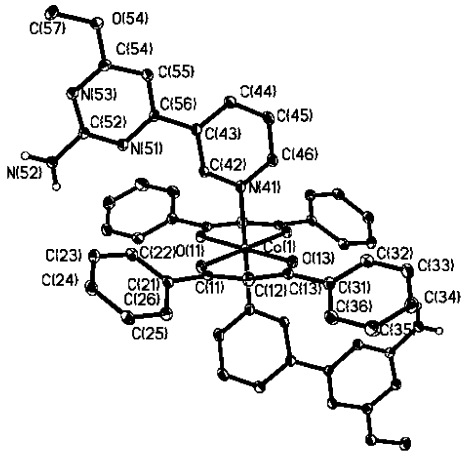

Figure 5. Labeled thermal ellipsoids in the crystal structure of **8** drawn at 50% probability level (hydrogen atoms, apart from $-NH_2$, omitted for clarity).

Crystallographic data are presented in Table 1, and relevant hydrogen-bond data are shown in Table 2.

Results

Ligands **1** and **2** were prepared in good yields via Pd-catalyzed Suzuki−Miyaura cross-coupling reactions, Scheme 1. Ligand **6** was prepared in good yields by means of the palladium-catalyzed Sonogashira coupling of 3-methoxy-5-ethynylpyridine with 2-amino-4-chloro-6-methylpyrimidine, Scheme 2. 3-Methoxy-5-ethynylpyridine was synthesized in excellent yields by means of Sonogashira coupling conditions of 3-methoxy-5-bromopyridine and (trimethylsilyl)acetylene followed by base-promoted deprotection.

The crystal structure of **7** contains two crystallographically unique complexes (A and B), Figure 3. The two py-pym ligands **1** reside perpendicular to the [$(hfac)_2Cu^{II}$] complex resulting in an octahedral coordination geometry around the copper center. The ligands are coordinated through the pyridyl nitrogen atoms with Cu−N distances of 2.0227(16) and 2.0049(15) Å, respectively. Due to the close similarities of the supramolecular assembly of A and B, only one will

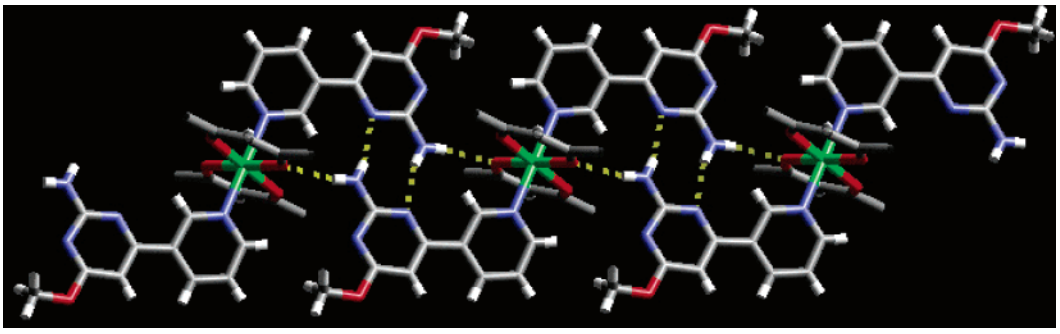

Figure 6. Infinite chain in the crystal structure of **8** produced from N−H···O and N−H···N hydrogen bonds. Acac phenyl rings have been omitted for clarity.

parameters, were included in the atom list. Atomic coordinates for the two amine hydrogen atoms, H22A and H22B, were allowed to refine.

10. The copper complex sits on a general position. A slight

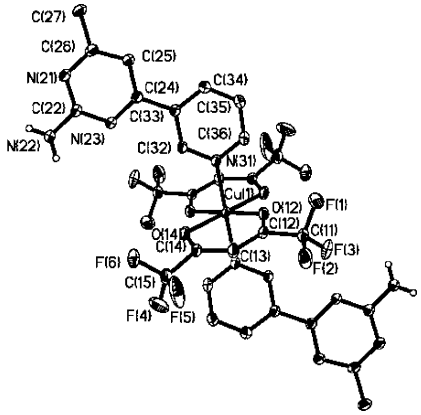

Figure 7. Numbered thermal ellipsoids in the crystal structure of **9** drawn at 50% probability level. One molecule of 1,2-dichloroethane and the hydrogen atoms (apart from $-NH_2$) have been omitted for clarity.

described in detail. Neighboring complex ions are held together in a head-to-tail motif by which the *syn*-amino proton forms a N−H···O hydrogen bond with an oxygen atom from an adjacent acac complex, producing an infinite ribbon, Figure 4. The *anti*-amino proton and the pyrimidine nitrogen atoms are participating in extending the networks. In addition, two molecules of chloroform are incorporated into the crystal lattice.

The metal complex in the crystal structure of **8** is composed of two py-pym ligands **1** bound at the axial positions of the [$(DBM)_2Co^{II}$] complex, Figure 5. The Co(II) ion displays an octahedral coordination geometry with a Co−N distance of 2.1514(14) Å. The extended network exhibits the same connectivity as that of **7**, in which head-to-tail N−H···O hydrogen bonds are formed between the

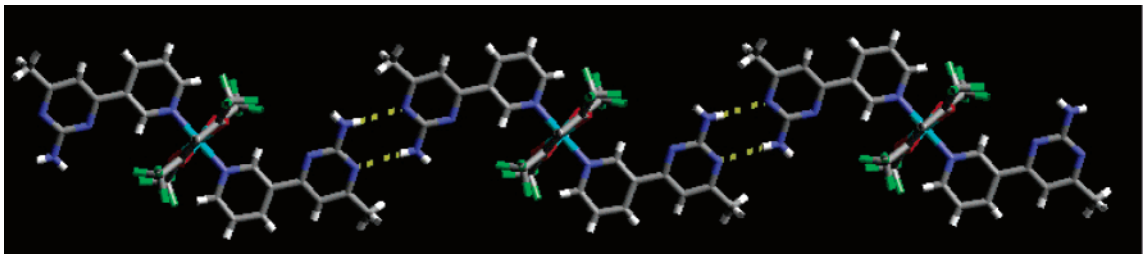

Figure 8. Infinite ribbon held together by self-complementary N−H···N aminopyrimidine interactions in the crystal structure of **9**.

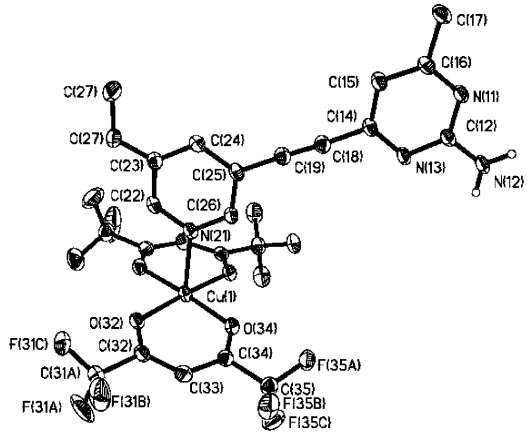

Figure 9. Labeled thermal ellipsoids (drawn at 50% probability level) of crystal structure **10** with the hydrogen atoms (apart from $-NH_2$) omitted for clarity.

anti-amino proton and an oxygen atom from a neighboring acac complex. Additionally this structure displays self-complementary N−H···N hydrogen bonds, between the *syn*-amino proton and a pyrimidine nitrogen atom, Figure 6.

The metal complex in **9** is composed of two py-pym ligands **2** bound to a [$(hfac)_2Cu^{II}$] complex. The orientation and arrangement of the py-pym ligands **2** with respect to the [$(hfac)_2$Cu(II)] complex are similar to those shown in the structure of **7**, where coordination to the axial positions of the metal ion takes place via the pyridyl moieties thus creating an octahedral metal environment with a Cu−N distance of 2.0044(12) Å, Figure 7. Within this arrangement the aminopyrimidine functionality is suitable for self-complementary hydrogen bonds with neighboring complexes. Thus the *syn*-amino protons form self-complementary N−H···N hydrogen bonds with pyrimidine nitrogen atoms resulting in a one-dimensional infinite ribbon, Figure 8. The

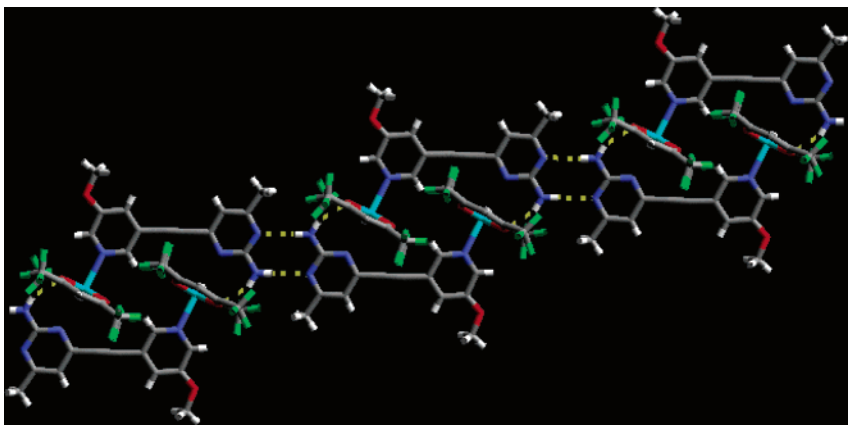

Figure 10. Extended network in the crystal structure of **10** showing the N−H···N and N−H···O hydrogen bonds.

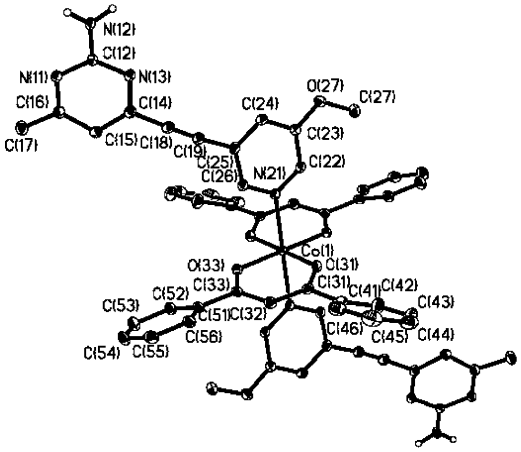

Figure 11. Labeled thermal ellipsoids of structure **11** drawn at 50% probability level with the hydrogen atoms (apart from $-NH_2$) omitted for clarity.

extended structures of **7** and **9** are possibly different due to a subtle change of the substituents on the organic counterpart. Ligand **1** has a methoxy substituent *ortho* to the pyrimidine nitrogen atom sterically congesting that binding site, thus blocking the interactions to the neighboring amino protons. The second pyrimidine nitrogen atom and *anti*-amino proton are not involved in extending the network. Furthermore a solvent molecule of 1,2-dichloroethane is incorporated in the crystal lattice, but disruption of the self-complementary hydrogen bonds does not occur.

The crystal structure of **10** includes only one py-pym ligand **6** coordinated to a $[(hfac)_2Cu^{II}]$ complex in the axial position, Figure 9. Coordination occurs through the pyridyl nitrogen atom of the ligand to the copper center with a Cu−N distance of 2.2751(18) Å, resulting in a square pyramidal metal coordination geometry. The ligand:metal complexes form head-to-tail N−H···O hydrogen bonded dimers through

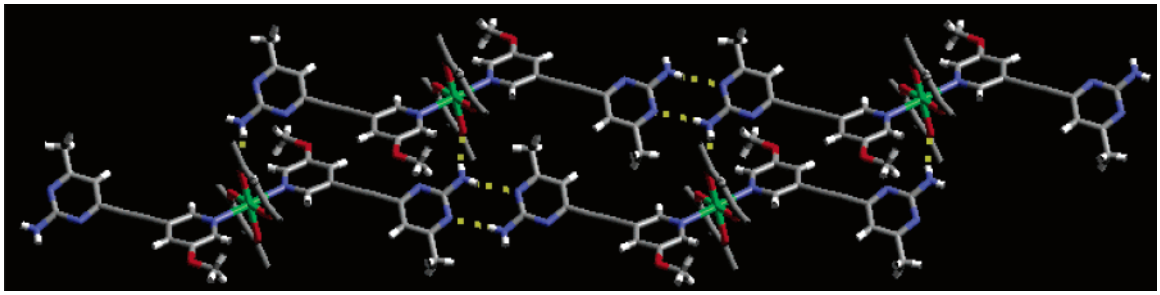

Figure 12. Extended network in the crystal structure of **11** with the phenyl rings omitted from the metal acac complex for clarity.

the *anti*-amino proton to the oxygen atom of an adjacent metal acac complex. Further extension of the network is fashioned by self-complementary N−H···N hydrogen bonds from the *syn*-amino proton to a nitrogen atom of the pyrimidine ring, Figure 10. The second pyrimidine nitrogen atom is aligned to coordinate at the axial position of a neighboring acac complex, although the Cu−N distance is approximately 2.70 Å.

The metal complex in **11** contains two symmetry-related py-pym ligands **6** bound axially to a $[(DBM)_2Co^{II}]$ complex with a Co−N bond distances of 2.2083(11) Å creating an octahedral cobalt coordination geometry, Figure 11. The network forms an infinite sheet by self-complementary N−H···N hydrogen bonds from the *syn*-amino protons to a nitrogen atom of the pyrimidine ring and by N−H···O hydrogen bonds from the *anti*-amino protons to an oxygen atom of the adjacent acac complex, Figure 12.

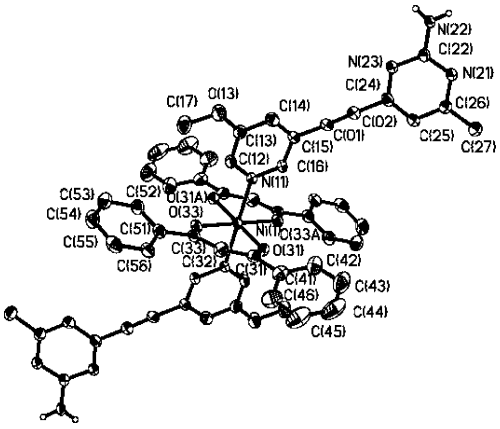

Figure 13. Labeled thermal ellipsoids for the crystal structure of **12** drawn at 50% probability level with the hydrogen atoms (apart from $-NH_2$) omitted for clarity.

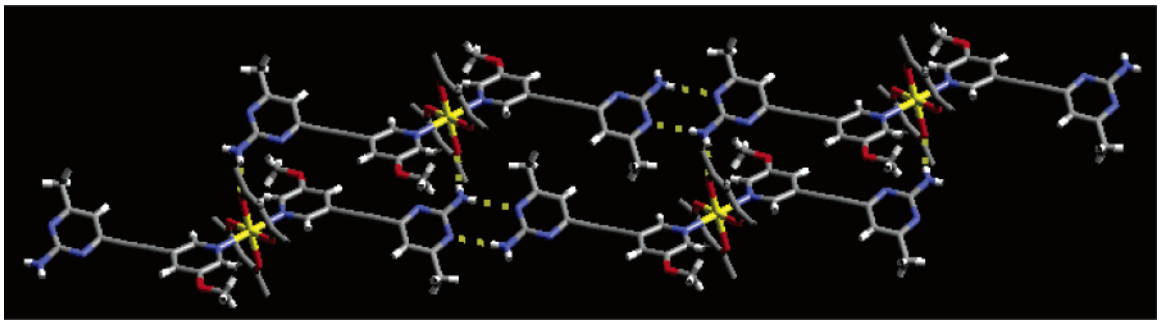

Figure 14. Extended network in the crystal structure of **12** with the phenyl rings omitted from the metal acac complex for clarity.

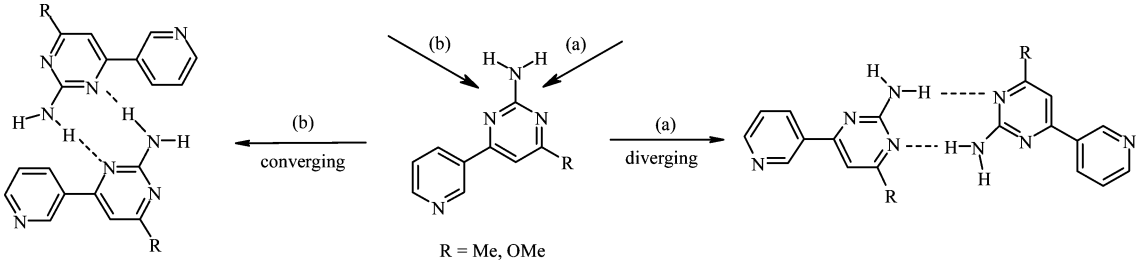

Figure 15. Pictorial explanation of diverging vs converging structural motifs.

The crystal structure of **12** is isostructural with the crystal structure of **11**. Two py-pym ligands **6** are coordinate axially to the $[(DBM)_2Ni^{II}]$ complex with Ni−N bond distances of 2.142(2) Å creating an octahedral coordination geometry around the nickel center, Figure 13. The overall structure is extended through self-complementary N−H···N hydrogen bonds from the *syn*-amino protons to a nitrogen atom of the pyrimidine ring and by N−H···O hydrogen bonds from the *anti*-amino protons to an oxygen atom of an adjacent acac complex, Figure 14.

Discussion

The decision to employ chelating ligands to control the coordination chemistry especially around the often unpredictable Cu(II) ion resulted in each case in complex ions with well-defined coordination geometry due to two acetylonate ligands bound in the equatorial positions. This configuration provides an open approach along the axial positions, which essentially creates a linear metal-containing building block, the geometry of which can be extended into an infinite 1-D assembly with the help of a suitable bifunctional ligand. The pyridyl moiety of the ligands **1, 2**, and **6** coordinates in each case to the metal ion, which typically generates an octahedral complex. The one exception is **10** where only one of the two axial positions is occupied by a pyridyl moiety resulting in a square-pyramidal Cu(II) geometry. The supramolecular chemistry in **7** and **8** does not work exactly as intended. In the former, the desired self-complementary N−H···N/N···H−N motif does not form, and in the latter, it does appear as intended but the interaction takes place on the side of the ligand that gives rise to a converging instead of a diverging motif, Figure 15.

The drawback with ligand **1**, at this stage, seemed to be that the methoxy substituent showed a propensity to orient itself in such a way as to limit intermolecular access to N(2). In fact, a search of the CSD showed that a methoxy substituent *ortho* to a pyridine nitrogen atom is very likely to reside coplanar with the ring and face the adjacent nitrogen atom, which does limit its availability as a potential hydrogen-bond acceptor.[15] To improve opportunities for the desired self-complementary N−H···N interaction, we replaced the methoxy substituent with a less intrusive $-CH_3$ group (resulting in ligand **2**). The crystal structure determination of **9** shows that a relatively minor molecular modification was needed to achieve the desired supramolecular assembly process; neighboring py-pym ligands are interconnected in a linear manner through the intended N−H···N/N···H−N motif, Figure 8.

Another way of minimizing steric crowding (that could prevent or disrupt intended supramolecular assembly) would be to increase the separation between the two different binding sites on the bifunctional ligand. Consequently, an ethynyl bridge was incorporated into **6** in an attempt to facilitate access to the hydrogen-bonding site and this strategy worked very well as exemplified by the crystal structure determinations of **10**−**12**. Despite the fact that the coordination chemistry is different, square-pyramidal vs octahedral, respectively, both contain the self-complementary hydrogen bonds between adjacent aminopyrimidine sites that act as the principle driving forces for the supramolecular assembly.

This study provides an outline for how a supramolecular strategy geared toward a very specific target can be refined and developed through a systematic structural study. The structural information provides direct feedback and thus guides the covalent modifications of the ligands that are required to optimize the supramolecular assembly process. The result is a structurally bifunctional supramolecular reagent, ligand **6**, that produces the desired supramolecular motif, infinite 1-D chains, in high yields. This study also serves to underscore some of the similarities between the development of noncovalent and covalent synthetic methodologies. In each case, the driving force is a specific goal, an individual molecule, or an assembly of molecules, respectively. The efficiency of the synthesis can be improved by systematically altering reaction conditions or by making deliberate changes to the supramolecular reagent.

Acknowledgment. Financial support from the NSF (Grant CHE-0316479) and Kansas State University is gratefully acknowledged.

Supporting Information Available: X-ray crystallographic data in CIF format and ^1H and ^{13}C NMR specta of ligands **1**−**3** (PDF). This material is available free of charge via the Internet at http://pubs.acs.org.

IC048405Y

(15) A CSD search resulted in 30 crystal structures showing a methoxy substituent *ortho* to the pyridine nitrogen. In all 30 structures the methoxy substituent is bent toward the nitrogen atom.